Materials Letters 139 (2015) 165–168

Contents lists available at ScienceDirect

Materials Letters

journal homepage: www.elsevier.com/locate/matlet

Fiber reinforcement during 3D printing

Susanne Christ, Martin Schnabel, Elke Vorndran, Jürgen Groll, Uwe Gbureck*

Department for Functional Materials in Medicine and Dentistry, University Hospital Würzburg, Pleicherwall 2, 97070 Würzburg, Germany

ARTICLE INFO

Article history:
Received 4 September 2014
Accepted 11 October 2014
Available online 23 October 2014

Keywords:
3D powder printing
Fibre reinforcement
Mechanical properties

ABSTRACT

Three-dimensional (3D) printing is an attractive rapid prototyping technology for the fabrication of 3D structures by the localized deposition of a reactive binder liquid onto thin powder layers in predominantly technical applications. A practical limitation is often the low green strength of printed samples, which can lead to a collapse of large and fragile structures during removal from the powder bed and the following depowdering procedure. Fibre reinforcement may improve green mechanical properties of printed samples, which was investigated in this study using a range of different short fibres added to a matrix of cellulose-modified gypsum powder. Mechanical testing of printed samples revealed a bending strength increase of 180% and up to 10 times higher work of fracture values compared to non-reinforced printed samples.

1. Introduction

Three-dimensional powder printing (3DP) is used to create 3D structures of complex shape by localized application of binder into a powder bed [1]. The great advantage of 3DP is an accurate control of the complex structure and a setting at room temperature. Hardening of the structures occurs by either using organic binders, which partially dissolve in contact with printing liquid and bind particles together after drying [2] or hardening can be achieved by using reactive powders showing a hydraulic setting reaction [3]. A practical limitation of 3D printing is the relatively low initial green sample strength, which can lead to a collapse of large structures during removal from the powder bed and the following depowdering procedure [4].

This study aimed at increasing the green strength of 3D printed parts by using a fibre reinforcement approach similar to mineral bone cements [5–8]. The major challenge for such an approach in 3D printing is the requirement to obtain smooth powder layers (~100–200 μm thickness) within the printer. This likely restricts the fibre length and the fibre volume ratio within the powder; in this study we investigated the effect of adding 1% short fibres with a maximum length of 1–2 mm to a matrix of cellulose-modified gypsum powder. The fibre length was limited by the printing process, as the addition of longer fibres prohibited the preparation of thin and smooth powder layers during printing. Nevertheless, the fibre length was likely above the critical length according to literature for fibre-reinforced ceramic matrix composites [9].

2. Materials and methods

3D printing of samples was performed on a ZPrinter 310 (ZCorporation, USA) with a layer thickness of 0.1 mm and a binder volume saturation of 100%. The powder for printing was prepared by mixing commercially available dental gypsum (GC Fujirock EP, Belgium) with 5% (hydroxypropyl)methylcellulose (Fluka) in a ploughshare mixer (M5R, Lödige, Germany) for 10 min. For reinforcement four different commercially available fibres were tested: polyacrylonitrile fibre fillers (PAN), polyacrylonitrile short cut fibre (PAN-sc), polyamide fibre fillers (PA), and alkali resistant zirconium silicate glass short cut fibre (glass fibre) (Heinrich Kautzmann, Germany). All fibres were separated by sieving through a 1 mm mesh size sieve before mixing with the powder for 10 min at a fibre content of 1%. Samples for bending tests (5 mm × 4 mm × 45 mm) were printed in two different orientations as shown in Fig. 1 and incubated for 20 h in water saturated atmosphere. Printing with *z* orientation was not performed because samples (with or without fibre addition) were not stable enough to be removed from the building chamber. Half of the samples were further infiltrated with a self-setting polyurethane resin (Axson technologies, Germany) for additional reinforcement. Mechanical properties were tested by four-point bending test with $n=10$ using a static mechanical testing device Zwick/Roell Z010 (Zwick GmbH&Co.KG, Ulm, Germany). The 2.5 kN load cell was employed

The mechanical properties were determined using a four-point bending test regime in both *x* and *y* printing direction, as it is known from previous studies that 3D printing will cause anisotropic mechanical performance of the samples [1].

* Corresponding author. Tel.: +49 931 20173550.
E-mail address: uwe.gbureck@fmz.uni-wuerzburg.de (U. Gbureck).

http://dx.doi.org/10.1016/j.matlet.2014.10.065
0167-577X/

for measurements at a constant cross head speed of 1 mm/min and a pre-load of 0.1 N. To calculate the work of fracture (wof), mechanical testing was stopped when sample was fractured or at a maximum displacement of 3%. Density measurements were performed by Mohr–Westphal balance based on Archimedean principle using the device Kern ABT 100-5 M (Kern & Sohn GmbH, Germany) ($n=3$). Porosity characteristics such as pore size distribution and total porosity were measured by mercury (Hg) porosimetry (PASCAL 140/440, Porotec GmbH, Germany) with $n=1$. Furthermore, fracture surfaces were examined using scanning electron microscopy (SEM) with a Digital Scanning Microscope DSM 940 (Zeiss, Germany) at an accelerating voltage of 5 kV. Statistical calculations were performed with ANOVA using the software SigmaPlot 12.5 (Systat Software, Inc., 2011).

3. Results

Samples for bending test were printed in two different orientations (Fig. 1) to investigate the influence of fibre orientation within the sample and the influence of binder application due to print head movement. The results for flexural strength showed significantly increased values (up to 180%) for most of the samples (Fig. 2A) with only the flexural strength of PA fibres printed in *y* direction being comparable to the reference. Regarding standard deviation there was no difference between printing orientations concerning flexural strength; wof calculated by the area underneath stress–strain curves recorded during bending test and the cross sectional area of the sample (Fig. 2B) showed a similar behavior like flexural strength. Apart from PA-reinforced samples, wof was also independent of printing orientation and a total increase of up to one order of magnitude could be obtained. Polyurethane infiltration of the samples increased both flexural strength (Fig. 2C) as well as wof (Fig. 2D) by 10- to 20-fold. After this treatment, however, fibre-reinforced samples showed no significantly higher values compared to unreinforced samples. Furthermore, fibre content for PAN-reinforced gypsum was optimized with respect to mechanical properties (Fig. 2E). Flexural strength could be further increased to more than 400% with a fibre content of 1.5% and decreased slightly until 2.5%. A higher fibre content was not printable.

Density and porosity of the composites can have a great influence on mechanical properties. The density, however, was not affected by fiber reinforcement (Table 1). In contrast, porosity of the samples decreased if samples were reinforced (Table 1), but fibre material had no significant effect on porosity and pore size distribution (Fig. 3). Furthermore, fracture surfaces (Fig. 3) showed fibre pull out as well as matrix residues on the fibre surfaces. PAN and PA fibres seemed to be deformed, whereas PAN-sc and glass fibres remained intact.

4. Discussion

Examination of mechanical properties by four-point bending test revealed higher flexural strengths and wof for reinforced samples (Fig. 2), indicating a transfer of mechanical load from matrix into the fibre as well as energy dissipation by frictional forces during fibre pull out [10] resulting in higher strains of the composite. The highest wof values were found for PAN-sc due to its length of 2 mm and therefore its higher surface. Taking into account results of Castilho et al. [1], it can be assumed that orientation of printed fibre-reinforced samples could have an influence on mechanical properties. However, for both flexural strength and wof, there was no difference between printing orientations when samples were fibre reinforced. Due to binder application initial strength of *x* orientated samples was lower than for *y* orientated ones. This binder effect was compensated as fibres are predominantly aligned in *x* direction such that the reinforcement for *x* orientation is enhanced compared to (initially stronger) samples printed in *y* direction. Polyurethane infiltration increased mechanical properties enormously but at the same time eliminated the influence of fibre reinforcement. This indicates for this system that polymeric post-hardening has a greater influence on mechanical properties than fibre reinforcement.

Further investigation concerned density and porosity of the reinforced samples (Table 1). Density of all samples did not vary with different fibres. As density of PAN, PAN-sc, and PA is much lower than that of the gypsum mixture (around 1.2 g/cm³), a lower overall density could be expected. However, composite density was not affected due to a low fibre content of 1%. In contrast, porosity could be decreased by fibre addition from 62% (no fibre) to a minimum of 56%. These values are in accordance with printed samples found in literature [11–13]. Reduced porosity could also have contributed to better mechanical properties such as flexural strength.

The fibre–matrix interface (Fig. 3) shows matrix residues on all fibre surfaces indicating good adhesion between fibre and gypsum matrix. Furthermore, fibre pull out can be confirmed, which is typical for polymeric fibres in ceramic matrices [10]. As fibre pull out and interface debonding are the main mechanisms of energy absorption [6], the high wof can be associated with the findings of SEM images. Prior to fibre pull out, fibre bridging of the opening

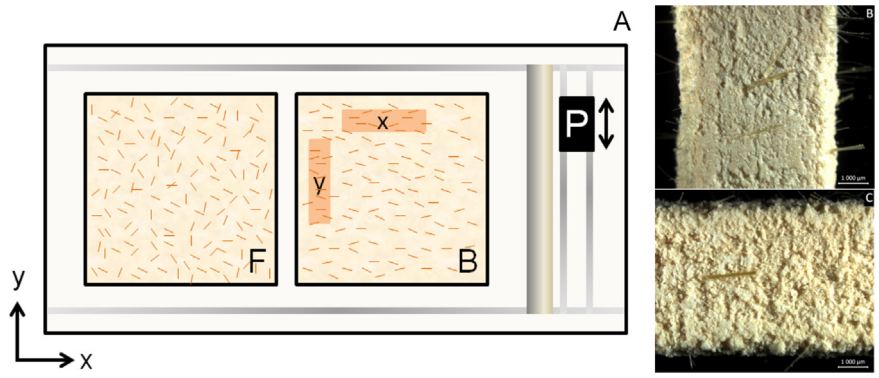

Fig. 1. Schematic top view of 3D printing (A). Feed chamber (F) and build chamber (B) are localized in *x*–*y* plane. Samples are labelled with *x* and *y* according to their orientation in the building chamber. The print head (P) moves across the building chamber in *x* direction where binder is sprayed in *y* direction (see arrow next to P). Figure B (*y* orientation) and C (*x* orientation) shows predominant fibre orientation within the samples.

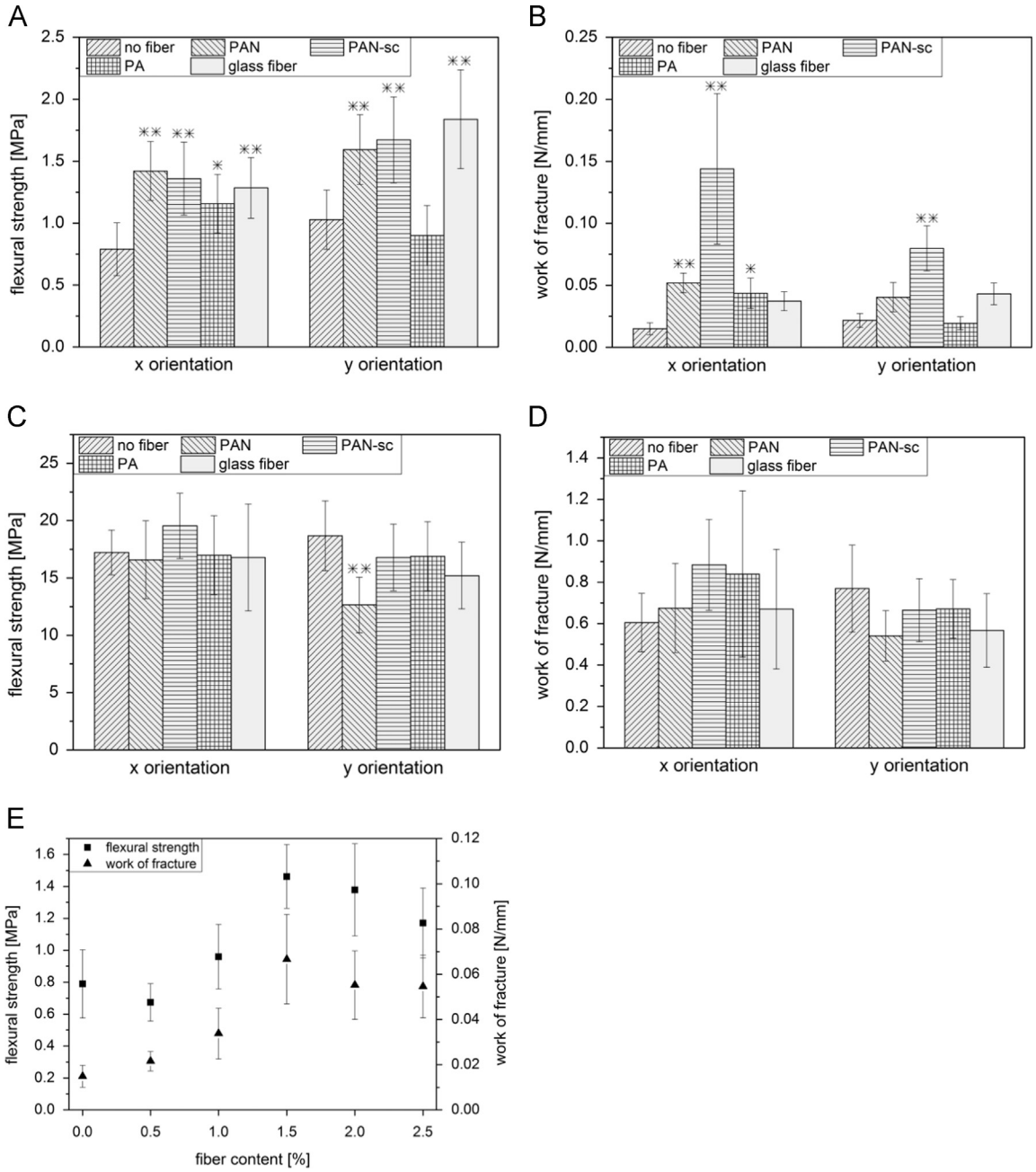

Fig. 2. Flexural strength (A) and wof (B) of fibre-reinforced samples printed in *x* and *y* direction. (C) Flexural strength and (D) wof of polyurethane infiltrated samples. Fibre content was optimized for PAN in *x* direction (E). Highly significant ($p < 0.01$) and significant ($p < 0.05$) samples are labelled with ** and *.

Table 1
Porosity and density of fibre-reinforced gypsum was measured with mercury porosimetry and Mohr–Westphal balance, respectively.

Fibre	Porosity (%)	Apparent density (mean ± SD) (g/cm^3)	Bulk density (mean ± SD) (g/cm^3)
No fibre	62.35	1.078 ± 0.010	2.10 ± 0.04
PAN	56.10	1.021 ± 0.002	1.95 ± 0.14
PAN-sc	59.10	1.089 ± 0.009	2.27 ± 0.06
PA	58.89	1.030 ± 0.004	2.13 ± 0.04
Glass fibre	57.82	1.060 ± 0.010	2.12 ± 0.01

crack leads to a higher deformation of the composite resulting again in a higher wof [6]. Moreover, PAN and PA fibres seem to be deformed, which can be ascribed to the manufacturing process of fibre fillers by grinding. Thus, no fibre fracture could be observed independent of fibre material and length.

5. Conclusion

We were able to introduce fibre reinforcement in 3D powder printing for the first time to improve green strength of complex samples. Despite a fibre length being one order of magnitude higher than the powder layer thickness during printing, fabrication quality of samples could be maintained during printing up to a fibre content of 2.5%. This study focused on materials (fibres and matrix) predominantly used in technical applications to demonstrate the principal reinforcement mechanism during 3D printing. A transfer of the results to biomedical applications, such as hard tissue replacement, would clearly require the use of biocompatible

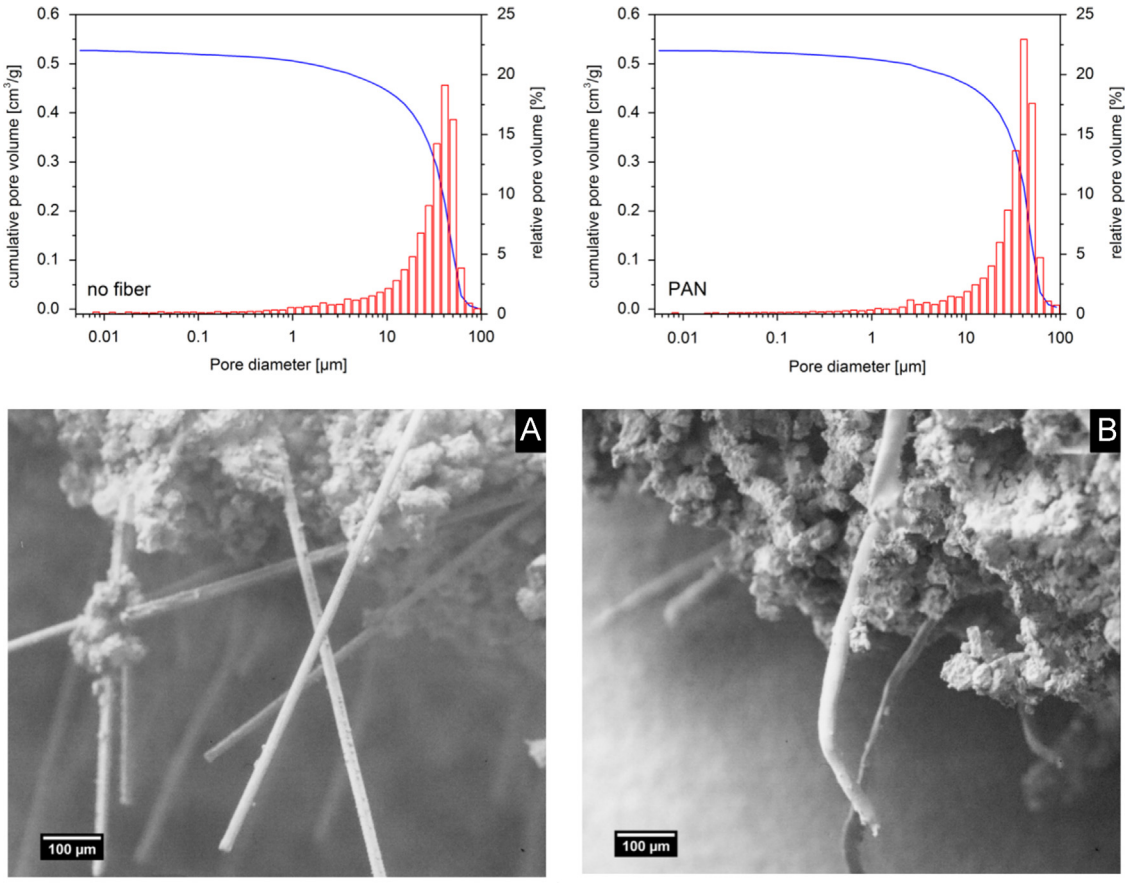

Fig. 3. Pore size distribution for gypsum without fibres and PAN-reinforced samples. SEM images (5 kV and 100 times magnification) show gypsum samples reinforced with PAN-sc (A) and PA (B), respectively.

and biodegradable fibres such as polylactic-co-glycolic acid as demonstrated before for fibre-reinforced mineral biocements [14].

References

[1] Castilho M, Dias M, Gbureck U, Groll J, Fernandes P, Pires I, et al. Fabrication of computationally designed scaffolds by low temperature 3D printing. Biofabrication 2013;5:035012.
[2] Seitz H, Rieder W, Irsen S, Leukers B, Tille C. Three-dimensional printing of porous ceramic scaffolds for bone tissue engineering. J Biomed Mater Res B Appl Biomater 2005;74B:782–8.
[3] Gbureck U, Hölzel T, Klammert U, Würzler K, Müller FA, Barralet JE. Resorbable dicalcium phosphate bone substitutes prepared by 3D powder printing. Adv Funct Mater 2007;17:3940–5.
[4] Salgado AJ, Coutinho OP, Reis RL. Bone tissue engineering: state of the art and future trends. Macromol Biosci 2004;4:743–65.
[5] Xu HHK, Quinn JB. Calcium phosphate cement containing resorbable fibers for short-term reinforcement and macroporosity. Biomaterials 2002;23:193–202.
[6] Krüger R, Groll J. Fiber reinforced calcium phosphate cements – on the way to degradable load bearing bone substitutes? Biomaterials 2012;33:5887–900.
[7] Gorst NJS, Perrie Y, Gbureck U, Hutton AL, Hofmann MP, Grover LM, et al. Effects of fibre reinforcement on the mechanical properties of brushite cement. Acta Biomater 2006;2:95–102.
[8] Zhang Y, Xu HHK. Effects of synergistic reinforcement and absorbable fiber strength on hydroxyapatite bone cement. J Biomed Mater Res A 2005;75A:832–40.
[9] Cheremisinoff NP. Handbook of ceramics and composites: mechanical properties and specialty applications. CRC Press; 1991.
[10] Li VC, Maalej M. Toughening in cement based composites. Part II: Fiber reinforced cementitious composites. Cem Concr Compos 1996;18:239–49.
[11] Butscher A, Bohner M, Hofmann S, Gauckler L, Müller R. Structural and material approaches to bone tissue engineering in powder-based three-dimensional printing. Acta Biomater 2011;7:907–20.
[12] Will J, Melcher R, Treul C, Travitzky N, Kneser U, Polykandriotis E, et al. Porous ceramic bone scaffolds for vascularized bone tissue regeneration. J Mater Sci Mater Med 2008;19:2781–90.
[13] Gbureck U, Hölzel T, Doillon CJ, Müller FA, Barralet JE. Direct printing of bioceramic implants with spatially localized angiogenic factors. Adv Mater 2007;19:795–800.
[14] Losquadro WD, Tatum SA, Allen MJ, Mann KA. Polylactide-co-glycolide fiber–reinforced calcium phosphate bone cement. Arch Facial Plast Surg 2009;11:104.